Water Resources Research

RESEARCH ARTICLE
10.1029/2020WR027221

Diurnal Pumped-Storage Operation Minimizes Methane Ebullition Fluxes From Hydropower Reservoirs

Jorge Encinas Fernández[1], **Hilmar Hofmann**[1], **and Frank Peeters**[1]

[1]Environmental Physics, Limnological Institute, University of Konstanz, Constance, Germany

Key Points:
- Draw down associated with turbination during pumped-storage operation triggers ebullition in reservoirs
- Continuous pumped-storage operation results in smaller ebullition than intensive pumping after long-term storage
- Appropriate management strategies can contribute to a reduction of greenhouse gas emissions from reservoirs

Supporting Information:
- Supporting Information S1

Correspondence to:
J. Encinas Fernández,
jorge.encinas@uni-konstanz.de

Citation:
Encinas Fernández, J., Hofmann, H., & Peeters, F. (2020). Diurnal pumped-storage operation minimizes methane ebullition fluxes from hydropower reservoirs. *Water Resources Research*, *56*, e2020WR027221. https://doi.org/10.1029/2020WR027221

Received 5 FEB 2020
Accepted 15 NOV 2020
Accepted article online 20 NOV 2020

Author Contributions:
Formal analysis: Jorge Encinas Fernández, Hilmar Hofmann, Frank Peeters
Investigation: Jorge Encinas Fernández
Writing – review & editing: Jorge Encinas Fernández, Hilmar Hofmann, Frank Peeters

Abstract Hydropower is considered green energy and promoted to reduce greenhouse warming. However, hydropower is typically generated using reservoirs and reservoirs are known to emit substantial amounts of the greenhouse gas methane (CH_4) to the atmosphere. In many reservoirs ebullition is the dominant pathway of CH_4 emission. We show that continuous diurnal pumped-storage operation, which combines water pumping into the reservoir typically during the night and water drawdown during high demand of electricity, is beneficial for reducing CH_4 ebullition associated with hydropower generation. This conclusion is based on ebullition fluxes and water levels measured over 3 months in Schwarzenbach reservoir located in Germany. The reservoir was managed using three modes of operation: (1) diurnal pumping and turbination, (2) no pumping and no turbination, and (3) diurnal turbination. Cross-correlation analysis indicates that ebullition fluxes predominantly occur during diurnal water level decrease associated with turbination. Consistently, average ebullition fluxes of CH_4 were negligible during Mode (2) and substantial during Modes (1) and (3). During Mode (3) the average CH_4 ebullition flux was ~197 mg $m^{-2}day^{-1}$, ~12 times larger than during Mode (1) (16 mg $m^{-2}day^{-1}$). Our data indicate that overall CH_4 ebullition is about 3 times larger during 51 days of operation consisting of 38 days of no turbination followed by 13 days of diurnal turbination than during 51 days of continuous diurnal pumped-storage operation. This suggests that continuous diurnal pumped-storage operation leads to reduced CH_4 ebullition from reservoirs and is therefore advantageous compared to modes of operations involving long-term, large-amplitude turbination cycles.

1. Introduction

Reservoirs are anthropogenic systems constructed to collect, store, and manage water by blocking the natural water flow of streams and rivers with artificial dams and/or by complex pumped-storage operation in artificial water systems. Reservoirs provide important services to society such as a reliable supply of drinking water, flood control, water for irrigation, hydroelectric power generation, and storage of energy (Lima et al., 2007). Each reservoir is managed according to the specific use of the system. The mode of operation typically consists of time periods during which water is accumulated in the reservoir and drawdown periods during which the water is withdrawn again. In case of hydroelectric power generation, the water is withdrawn through turbines (called turbination). Some hydropower reservoirs are designed as pumped-storage systems in which water is pumped from a reservoir at a lower elevation during low energy demands and turbinated during periods of peak energy demand. Pumped-storage hydropower plants are considered to be the most efficient systems to store electric energy (Kobler et al., 2019) and may play an important role in the management of renewable energy. The number and size of hydroelectric power reservoirs, and especially of pumped-storage systems, have increased substantially during the last years (Barbour et al., 2016; Deane et al., 2010; Rehman et al., 2015; REN21, 2017) to satisfy the increasing demand of energy and energy storage and the requirement to reduce greenhouse gas (GHG) emissions linked to energy production (Barbour et al., 2016; Commission, 2011; Ibrahim et al., 2008; Kobler et al., 2019). Hydroelectric energy has traditionally been considered green energy because its production seems free of GHG emissions to the atmosphere (Hoffert et al., 1998; Victor, 1998), and hydropower is therefore promoted as a climate neutral alternative energy source to fossil energy.

However, inland waters and thus also reservoirs are important components of the regional and global carbon cycle (Battin et al., 2009; Tranvik et al., 2009) and have been identified as an important source of atmospheric GHGs in the global budgets (Abril et al., 2005; Barros et al., 2011; Beaulieu et al., 2014; Hertwich, 2013; Luyssaert et al., 2012; Raymond et al., 2013). Reservoirs are known to accumulate large amounts of

fine-grained sediments and organic material and potentially act as important storage of terrestrial carbon (Clow et al., 2015; Mendonça et al., 2017; Phyoe & Wang, 2019). Because methane (CH_4) and carbon dioxide are major products of the carbon metabolism, reservoirs and impounded river sections are known to be potential hot spots of GHG emission (Deemer et al., 2016; Harrison et al., 2017; Maeck et al., 2014; Varadharajan & Hemond, 2012) and may contribute a major fraction of the global anthropogenic GHG emissions (Deemer et al., 2016; Hertwich, 2013).

CH_4 is mainly produced in anoxic sediments, and most of the CH_4 is stored in anoxic pore water or in anoxic water bodies (Bastviken et al., 2008). In oxic waters, CH_4 is typically oxidized at the sediment surface and the diffusive transport of CH_4 from the sediments into the water column is then rather small (e.g., Bastviken et al., 2002). Compared to the diffusive CH_4, flux from the sediments ebullition can be a much more efficient pathway for the transport of CH_4 from the sediments, as this process can bypass CH_4 oxidation at the sediment surface. CH_4 fluxes due to ebullition can contribute a large fraction of the overall CH_4 fluxes to the atmosphere from small- to medium-sized lakes (Bastviken et al., 2004, 2011; Joyce & Jewell, 2003; McGinnis et al., 2006). According to DelSontro et al., 2010, Sobek et al., 2012, and Maeck et al., 2014 ebullition is in many cases the major emission pathway of CH_4 from reservoirs.

Water level declines in natural inland water bodies and in reservoirs are typically associated with enhanced ebullition and thus with enhanced CH_4 emissions (Deborde et al., 2010; Engle & Melack, 2000; Harrison et al., 2017; Maeck et al., 2014; Varadharajan & Hemond, 2012). The reason is that a decrease in water level results in a decrease in hydrostatic pressure at the sediment surface which increases the likelihood that the equilibrium pressure of the gas stored in the sediments exceeds the ambient pressure. The latter is a prerequisite for the formation of a gas phase in the sediments and thus for the occurrence of ebullition. Substantial water level changes are a typical consequence of reservoir operation and are therefore a characteristic feature of reservoirs that is uncommon in lakes (Hayes et al., 2017). Most studies on ebullition fluxes in reservoirs have focused on the consequence of substantial reservoir drawdown in fall demonstrating that the level changes during this time period cause strongly enhanced ebullition and associated CH_4 fluxes that are substantially larger than during the rest of the year (Harrison et al., 2017; Ostrovsky et al., 2008; Scandella et al., 2011; Varadharajan & Hemond, 2012; Zohary & Ostrovsky, 2011). However, not only large level changes during drawdown over several days and weeks can enhance ebullition fluxes of CH_4 but also short-term level fluctuations connected to, for example, ship-lock operation (Maeck et al., 2014) or daily water drawdowns in reservoirs with hydroelectric power production (Harrison et al., 2017).

Because pumped-storage hydropower is up to now the most efficient way to store electric energy at intermediate time scales, reservoirs with pumped-storage operation will remain an important component in an energy concept based on renewable energy from solar and wind energy. We, therefore, address here the question whether pumped-storage operation can be optimized to reduce the emissions of CH_4 by ebullition. Specifically, we investigate whether it is advantageous to operate pumped-storage systems using frequent subdaily pump-turbination cycles with small amplitudes or using long-term, large-amplitude pump-turbination cycles with several days of pumping followed by substantial drawdown over several days.

Our investigation is based on data on CH_4 fluxes due to ebullition from the sediment in a pumped-storage hydropower reservoir that were measured over a time period of 3 months at a high temporal resolution (1 min). The mode of operation of the reservoir changed during the 3 months of observation which enabled us to investigate the implications of reservoir operation on ebullition and associated CH_4 fluxes in hydropower reservoirs. Specifically, the change in reservoir management (operation modes) caused a change in water level dynamics. This allowed a comparison of CH_4 ebullition fluxes during time periods with different water level fluctuation patterns within the same reservoir. Based on these results, we compared the CH_4 ebullition flux during continuous pumped-storage operation with that during intensive turbination after long-term storage.

2. Methods

The study was conducted in Schwarzenbach reservoir (48°39.334′N, 8°19.630′E), located in the southwest of Germany at about 660 m above sea level (a.s.l.). The reservoir has a surface area of ~0.6 km^2 and a maximum depth of 65 m (mean depth 21.8 m) at maximum capacity (~1.44×10^7 m^3). The basin has a steep V shape

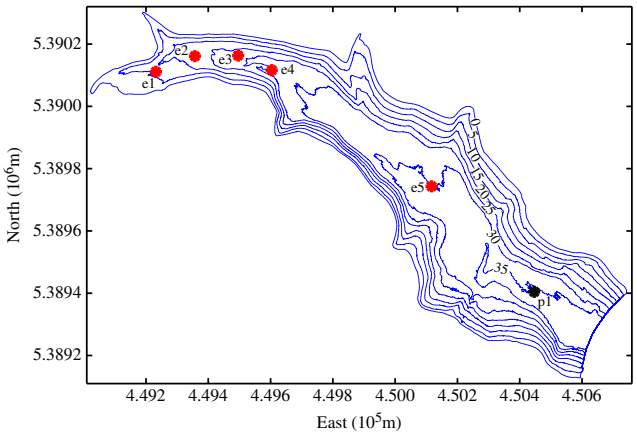

Figure 1. Bathymetric map of Schwarzenbach reservoir including the location of the different ebullition flux funnels (red points) and the profiling station (black point).

(see isolines in supporting information (SI) Figure S1), with minimum depths in the northwestern part, where the major natural inputs enter into the reservoir (Seebach and Schwarzenbach rivers), and maximum depth in the southeastern part, where the reservoir dam is located. Schwarzenbach reservoir is a pumped-storage hydropower system; that is, the water is pumped from Kirschbaumwasen reservoir during low energy demands and withdrawn through turbines located in Forbach to generate electric power (see SI Figure S1). During periods of turbination, the water level is drawn down whereas during pumping operation the water level increases. Water inlet and outlet for the pumped-storage operation is close to the dam in the deepest 5 m of the reservoir. Schwarzenbach reservoir receives additional water from a catchment area in the southwest of the reservoir by an artificial channel entering the reservoir at the southwestern shore. This water enters the reservoir at the water surface.

Between 13 and 28 July 2016, five ebullition flux funnels (EFF) were deployed ~1 m above the sediment along the thalweg at different water column depths (Stations e1–e5, Figure 1). After this initial experiment, the EFF located at Position e2 (Figure 1) remained at the same position until the end of October. Additional funnels were installed at Stations s1, s3, and s4 (see SI Figure S2). However, these funnels failed several times such that we have a long-term time series covering all three modes of operation only at Station e2.

At each of the EFFs water temperature and absolute pressure were measured at a frequency of 30 s (Aquatec AquaLogger 520). The pressure data were averaged to 1-min time resolution, and the water column height, *wl*, above the EFFs was calculated using the surface pressure measured during monthly gas sampling and batteries exchange when the EFFs were lifted to the water surface. The *wl* was used to calculate the rate of change in water level $wlc = dwl/dt$.

The EFF are inverted squared funnels that collect bubbles released from the sediment and guide the bubbles into a cylindrical column in which the gas displaces the water (see SI Figure S3). The volume of the collected gas is determined from the cross-section $A_c = \pi\, r_c^2$ of the cylindrical column with radius r_c and the column height h_c occupied by the gas. The height of the gas column is proportional to the difference between the hydrostatic pressure in the ambient water and the pressure within the column at the same depth. Differential pressure was measured with a differential pressure sensor at a sampling interval of 16 Hz. The time series of differential pressure was averaged to a temporal resolution of 1 min that was used in further statistical analysis. The height of the gas column, h_c, was estimated from these data using a linear calibration as presented in Maeck et al., 2014. The gas flux due to ebullition, *ef*, was calculated from the relation

$$ef = \frac{1}{A_f} A_c \cdot \frac{dh_c}{dt} \cdot \frac{p \cdot T_s}{p_s \cdot T} \tag{1}$$

where A_f is the area of the opening of the funnels parallel to the sediment, p and T are the hydrostatic pressure and temperature at the water depth of the funnel, and p_s and T_s are standard pressure (1 atm) and standard temperature (273.15 K). The ebullition fluxes *ef* calculated with Equation 1 provide the total volume of gas at standard conditions emitted by ebullition per unit area of sediment per unit time. For our funnels $A_f = 0.64$ m^2 and $r_c = 1.5$ cm.

During monthly campaigns, the batteries of the EFF were exchanged and gas samples were taken from the gas phase accumulated in the collecting columns. Water samples for analysis of dissolved CH_4 in the water column were taken regularly at 1-m water depth and on 12 July, 16 August, 13 September, and 13 October at different water depths at the Station p1 (Figure 1).

The water samples were collected using a 2-L water sampler (Limnos, Rossinkatu 2 E17, Turku, Finland) and transferred into 122-ml serum bottles that contained salt and were vacuumed before sampling. For details on the sampling procedure see Hofmann et al. (2010). The CH_4 concentration in these water

Table 1
Details for Each of the Selected and Analyzed Time Sections

Section	Type of operation	Mean temperature (°C)	Mean water depth (m)	Mean water level (m a.s.l.)	Lowest water level (m a.s.l.)	Highest water level (m a.s.l.)
1 (7–11 Aug.)	Diurnal pumping and turbination	14.38	10.57	659.07	658.91	659.29
2 (5–9 Sep.)	No pumping and no turbination	14.73	10.77	659.27	659.12	659.34
3 (13–18 Oct.)	Diurnal turbination	13.07	10.9	659.40	659.11	659.70

Note. Data are based on measurements at Station e2 (Figure 1).

samples was measured using the headspace technique. The gas samples from the EFF and the gas extracted from the head space of the water samples were analyzed for CH_4 using a gas chromatograph with a flame ionization detector (Shimadzu GC-9A). The GC was calibrated using gas standards of 10, 50, and 100 ppm (Air Liquide). The measurements of triplicate samples varied on average by <5%. Parallel to the water sampling, vertical profiles of temperature and dissolved oxygen (DO) were measured with a multiparameter probe (CTD probe, RBR Ltd., Ottawa, Canada; fast oxygen optode 4330F, AANDERAA, Bergen, Norway) at a sampling frequency of 6 Hz.

The relation between ebullition flux and total hydrostatic pressure was assessed using the fluxes measured by the five EFFs deployed along the thalweg at different water column depths (Figure 1).

The implications of different modes of operation of the reservoir on ebullition fluxes were investigated by comparing water level fluctuations and ebullition fluxes measured at Station e2 (Figure 1) because this is the only station for which we have ebullition fluxes during all three modes of operation of the reservoir. Detailed analysis is based on three time periods each covering 5 days (Table 1): Section 1 (7–11 August), Section 2 (5–9 September), and Section 3 (13–18 October). These time periods were selected because they are characterized by (i) similar water levels (658.9 to 659.7 m a.s.l.) implying similar mean water column height above the sediment (~10.8 m at Station e2) and thus similar mean hydrostatic pressure, (ii) similar water temperatures (13.07 to 14.73°C) implying similar production and oxidation rates of CH_4, and (iii) different reservoir operation modes (Table 1).

Temporal patterns in the time series of the rate of water level change and of ebullition fluxes were investigated using the autocorrelation of each of these time series. Cross correlation between these two time series was employed to investigate the relationship between the rate of change in water level and the ebullition flux at Station e2. Data series were detrended prior to the correlation analysis, and the MATLAB function corrcoef was used for the determination of correlation coefficients.

The Anderson-Darling test was used to evaluate whether the ebullition flux followed a normal distribution or not. The Kruskal-Wallis test was used to assess whether different data sets originated from the same distribution. Both tests were performed using the adtest and Kruskal-Wallis functions from MATLAB.

In addition to ebullition fluxes we determined diffusive CH_4 fluxes at the water surface of the reservoir from CH_4 concentrations and water temperatures measured at 1-m water depth and wind speed measurements at the dam of the reservoir. Diffusive CH_4 fluxes were estimated using the gas transfer velocity of Cole and Caraco (Cole & Caraco, 1998) and the Schmidt number dependence of the gas transfer velocity (Liss & Merlivat, 1986; for details see Encinas Fernandez et al., 2014).

3. Results

3.1. Water Column Dynamics

Between July and September 2016, the reservoir was stably stratified as is indicated by the decrease of the water temperature with increasing depth (Figure 2a). On 11 October, the water temperature was almost constant in the entire column (Figure 2a) suggesting that at least partial mixing of the water column had occurred. During the entire measuring period, dissolved O_2 concentrations were highest in the upper 2 m and decreased with increasing depth. The values just above the sediment were DO ~7 mg L^{-1} in July and

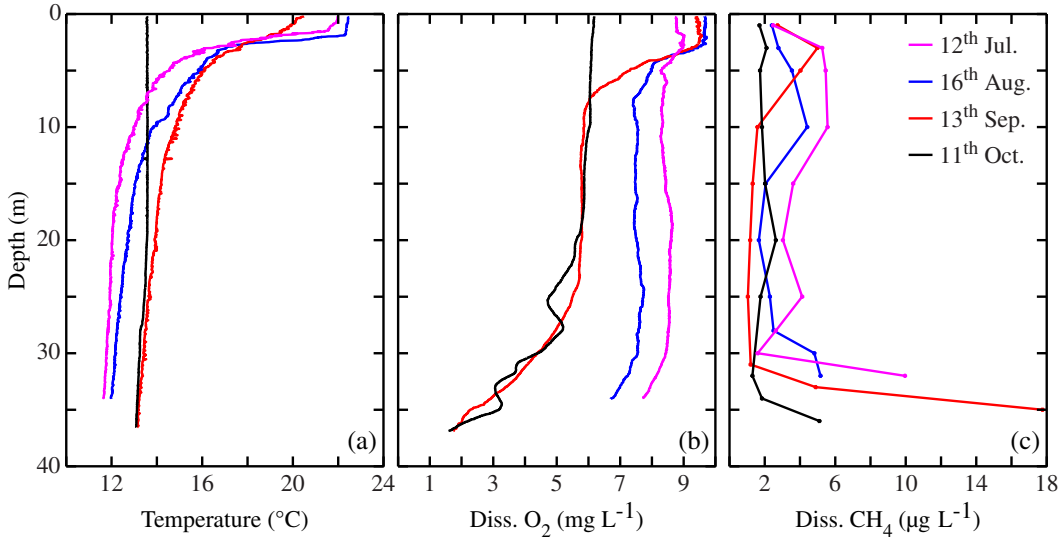

Figure 2. Profiles of (a) temperature, (b) dissolved O_2, and (c) dissolved CH_4 measured at the deepest Station p1 (Figure 1).

August and DO ~2 mg L^{-1} in September and October, indicating oxic conditions throughout the water column during the entire measuring period (Figure 2b). In all profiles dissolved CH_4 concentrations were below 6 µg L^{-1} throughout the water column except for the deepest sampling points in July and in September, where the CH_4 concentration was increased near the sediment (Figure 2c). The near surface concentrations of CH_4 between April and November 2016 measured at Station p1 at 1-m water depth ranged between 1 and 3 µg L^{-1} and the diffusive fluxes of CH_4 ranged between 0.6 and 1.8 mg CH_4 m^{-2} day^{-1} (see SI Figure S4).

3.2. Spatial Variability of Ebullition Along the Thalweg

During the initial deployment of the EFFs (Figure 1), the average ebullition flux decreased along the thalweg of the reservoir from the backwater in the northwest to the dam in the southeast (Figure 3). Ebullition fluxes were highest at shallowest sites and small at larger water depths (Figure 3). The 15-day average of *ef* at Station e1 (water column depth 5 m) was ~86 ml m^{-2} day^{-1} whereas the 15-day average *ef* at Station e2 (water column depth 10.5 m) was only ~54 mL m^{-2} day^{-1}. The gas collected in the funnels contained 56% CH_4 at Station e1 and 44% CH_4 at Station e2. Hence, the ebullition flux was 48 ml CH_4 m^{-2} day^{-1} at e1 and 24 ml CH_4 m^{-2} day^{-1} at e2. At standard conditions the molar gas volume is 22.41 L mol^{-1}, and 1 ml CH_4 therefore corresponds to 4.46×10^{-5} mol CH_4 or 0.716 mg CH_4. The ebullition flux of CH_4 therefore is ~35 mg CH_4 m^{-2} day^{-1} at e1 and ~17 mg CH_4 m^{-2} day^{-1} at e2. At all other stations, at which the water column depth exceeded 15 m, essentially no ebullition fluxes were observed (Figure 3).

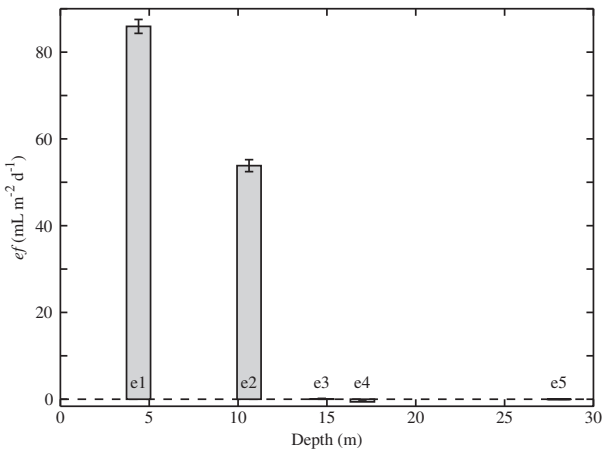

Figure 3. Ebullition fluxes in relation to water column depth during 13 and 28 July 2016 at the Schwarzenbach reservoir. The ebullition flux was standardized to 1 atm and 273.13 K.

3.3. Temporal Variability of Ebullition at the Station e2

During the study period from July to October, the water level showed different patterns of water level change (Figure 4a). Between 13 July and 22 August, water level fluctuations were characterized by reoccurring short-term decreases and increases of the water level by ~20 cm at subdaily time scales (Figure 4a). The water level changes are caused by diurnal pumping and turbination (Operation Mode 1) typical in reservoirs used for hydropower generation; that is, water level drawdowns occurred in the evenings and at some days in the morning too due to turbination of water for energy production, and level rises occurred during the nights

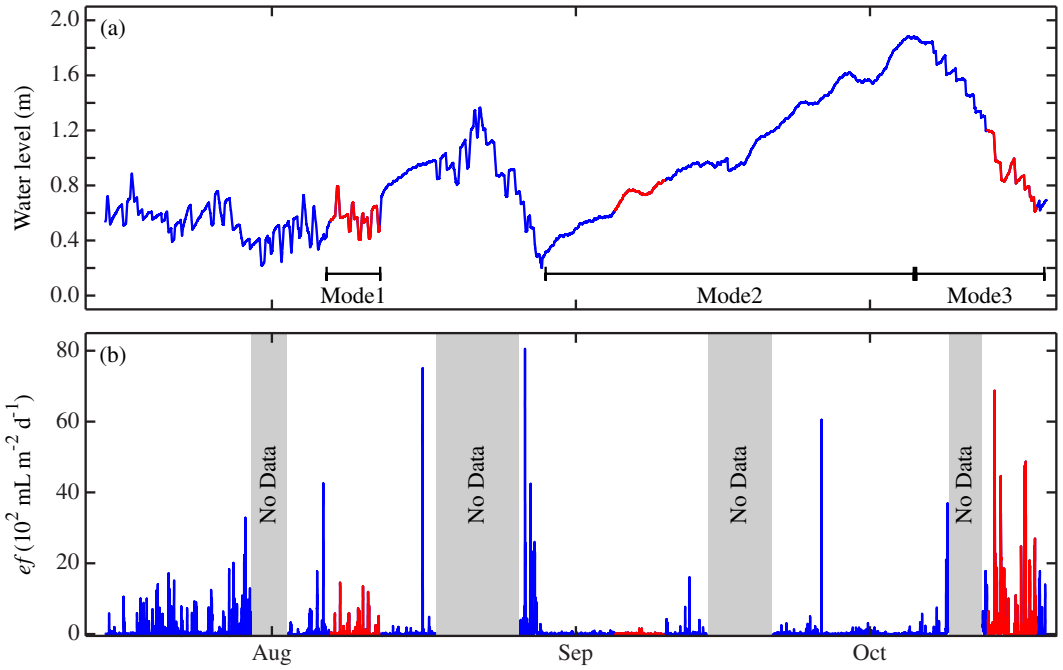

Figure 4. Water level (a) and ebullition flux (b) dynamics from July until the end of 2016 at the Schwarzenbach reservoir. The water level is relative to a reference water level of 658.5 m a.s.l., the minimum water level found during the pumped-storage operation mode of the Schwarzenbach reservoir. The ebullition flux is based on data collected at Station e2 (Figure 1). The red sections correspond to the three specific time periods selected (Figure 5). Note that the large peak in late September is generated by a single sampling point.

due to pumping of water into the reservoir, here from Kirschbaumwasen reservoir (see SI Figure S1). During this time period of diurnal pumped-storage operation, the average ebullition flux from the sediment was ~65 ml m^{-2} day^{-1}.

From 22 to 28 August, the reservoir operation was characterized by turbination of water once a day causing a drawdown in water level by ~18 cm day^{-1} (Figure 4a). The ebullition flux was only measured from 26 to 28 August. During these 3 days, the ebullition flux was ~513 ml m^{-2} day^{-1}. After 28 August, the management changed to no pumping and no turbination (Operation Mode 2). This management resulted in an essentially constant rise of the water level at an average rate of ~4.6 cm day^{-1} (Figure 4a). The ebullition flux was only ~11 ml m^{-2} day^{-1} during this time period. The highest water level was reached on 5 October when turbination was restarted. From 5 to 20 October reservoir management aimed at hydroelectric power production from the water stored during the previous period when the turbines were not operational. Similar to the last period in August, the reservoir operation was characterized by turbination of water typically once a day that was not followed by pumping water back into the reservoir (Operation Mode 3). As a consequence, the water level decreased over this time period by ~8.6 cm day^{-1} whereby the long-term decrease resulted from short periods of rapid drawdown followed by a rather constant level after the drawdown. Between 5 and 20 October, the ebullition flux was on average ~303 ml m^{-2} day^{-1}.

The implications of different reservoir operation modes on the CH_4 flux (Figures 5b1–5b3 and 5c) due to ebullition were investigated in detail by focusing on three time periods (Sections 1–3, Figure 5) representing the different patterns of water level changes (Figures 5a1–5a3) associated with the three modes of reservoir operation: (1) diurnal pumped-storage operation, (2) no pumping and no turbination, and (3) diurnal turbination but no pumping (Figures 5b1–5b3).

During Section 1, that is, between 7 and 11 August, the water level typically showed maxima during the day and minima during the night (Figure 5a1). The absolute change in water level averaged over a day was close to zero, but within a day the water level increased and decreased several times (Figure 5a1). During Section 1,

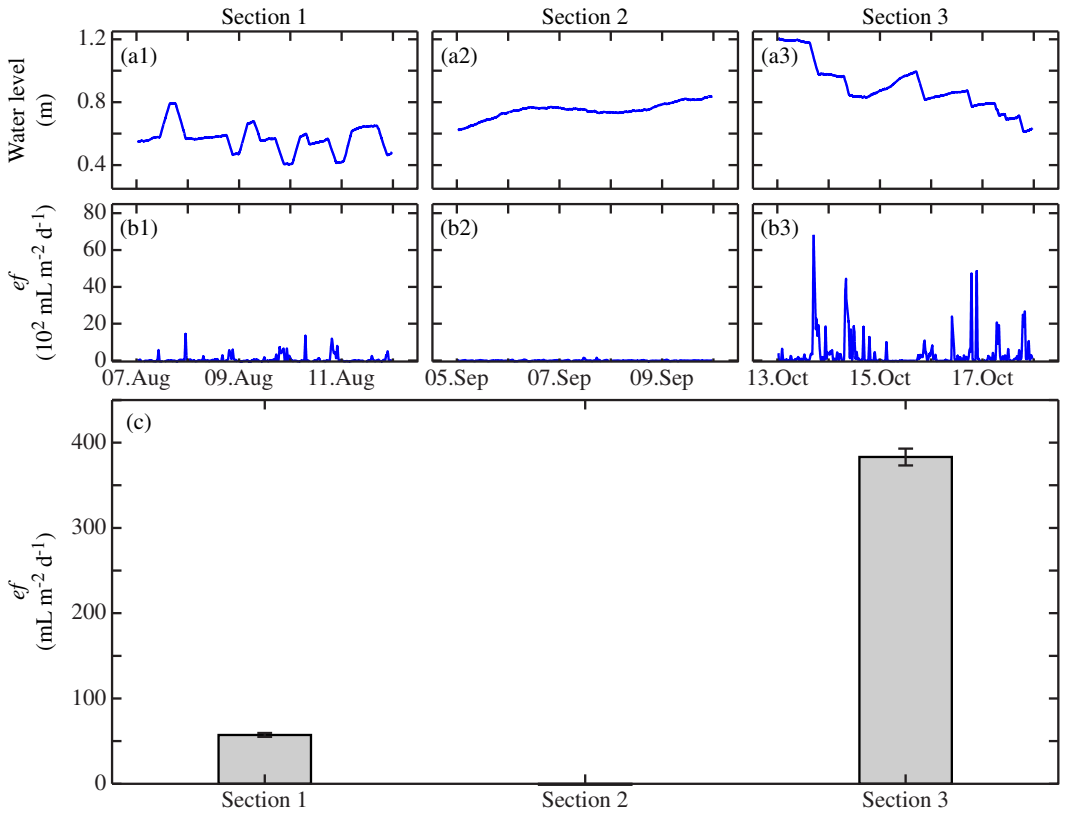

Figure 5. Water level (a) and ebullition flux (b) dynamics and average ebullition flux (c) during the three specific time sections representing the three different modes of operation (1) diurnal pumping and turbination, (2) no pumping and no turbination, and (3) diurnal turbination. The water level is relative to the reference water level of 658.5 m a.s.l.

the rate of change in water level, *wlc*, covered a wide range of negative and positive water level changes (−130 to 130 cm day^{-1}; Figure 6a1). The rate of water level change showed significant positive autocorrelations ($R = 0.6$, $p < 0.001$) at a lag of 24 hr (Figure 7a1) indicating daily reoccurrence of similar patterns in the water level fluctuations. The rate of water level change also showed a significant negative autocorrelation at a time lag of 6 hr ($R = -0.5$, $p < 0.001$), indicating a regular occurrence of one operation

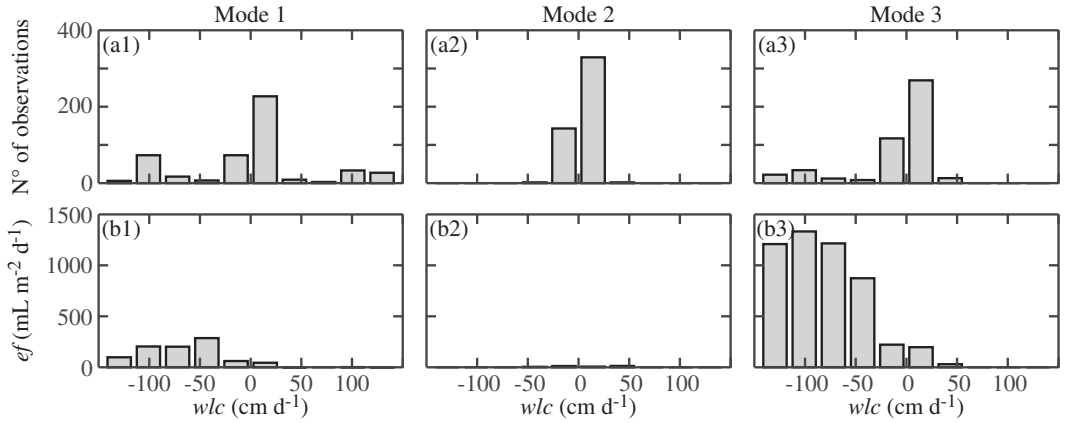

Figure 6. Histograms of the number of observations (a) and ebullition fluxes (b) as a function of the rate of change in water level, *wlc*, for the three specific time sections representing the three different modes of operation (1) diurnal pumping and turbination, (2) no pumping and no turbination, and (3) diurnal turbination.

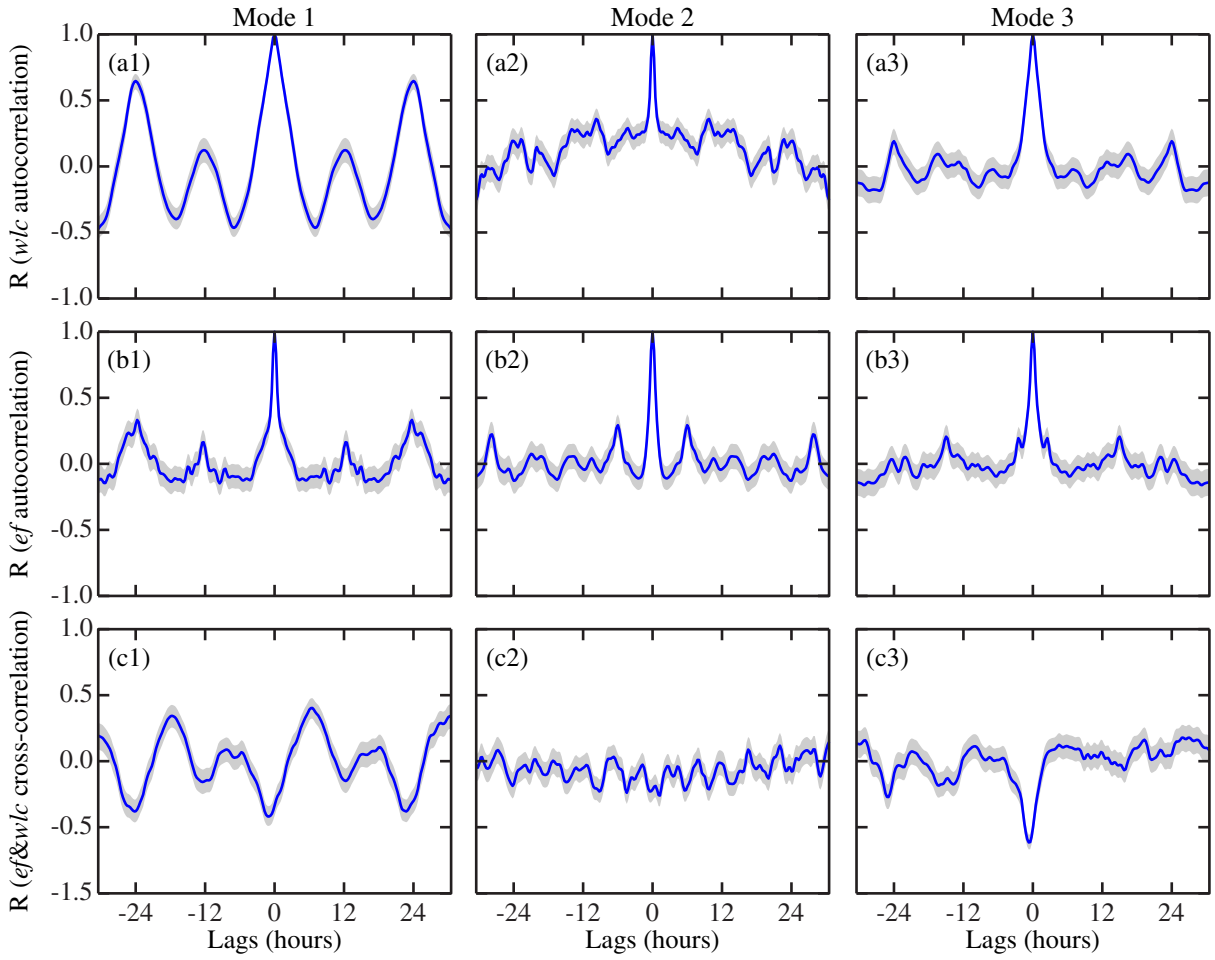

Figure 7. Autocorrelation of *wlc* (a) and of ebullition flux (b) and cross-correlations between *wlc* and ebullition flux (c) during the three specific time sections representing the three different modes of operation (1) diurnal pumping and turbination, (2) no pumping and no turbination, and (3) diurnal turbination. Autocorrelation and cross correlation are based on 15-min averages of *wlc* and ebullition flux. In the case of the cross correlations, the lags indicate a shift of ebullition flux relative to *wlc*.

cycle with 6-hr duration. The average *ef* during Section 1 was ~54 ml m^{-2} day^{-1} total gas (Figure 5c). The gas collected in the funnels contained 42% CH_4. Hence, the ebullition flux of CH_4 was ~16 mg CH_4 m^{-2} day^{-1}. Ebullition occurred mainly during negative *wlc* (Figure 6b1). This observation is supported by the cross correlation of *ef* and *wlc* indicating a significant negative correlation coefficient at a time lag of −1 hr ($R = -0.41$, $p < 0.001$, Figure 7c1). This significant negative correlation occurs periodically with a time period of 24 hr indicating a daily reoccurrence of ebullition events 1 hr after water level decreases. The cross-correlation analysis shows also a significant positive correlation ($R = 0.4$, $p < 0.001$, Figure 7c1) between *ef* and *wlc* at a time lag of 7 hr, that is, 6 hr after the negative correlation.

From 5 to 9 September (Section 2 and Figure 5a2) the water level increased on average by ~5 cm day^{-1} (Figure 6a2) without diurnal fluctuations. This pattern of water level change is reflected in the *wlc* autocorrelation showing no significant periodic cycling (Figure 7a2). The ebullition flux was on average *ef* ~0 ml m^{-2} day^{-1} total gas, thus substantially smaller than the ebullition flux during Time Period 1 (Figure 5c). Due to the low ebullition flux during Time Period 2 (Section 2), it was not possible to measure the proportion of CH_4 in the gas collected in the funnels. The *ef* and *wlc* during this period were not significantly correlated (Figure 7c2).

During Section 3 (13–18 October), the water level decreased (Figure 5a3) on average at a rate of about −11 cm day^{-1} (Figure 6a3). The long-term decrease in water level was mainly caused by several

short-lasting drawdowns in water level. The autocorrelation of *wlc* did not show a daily pattern (Figure 7a3) indicating that the short-term events during Section 3 did not occur at a consistent diurnal pattern. As during Section 1 ebullition during Section 3 was strongly linked to the sporadic events of water level drawdown, as is indicated by the significant negative cross correlation between *ef* and *wlc* ($R = -0.6$, $p < 0.001$; Figure 7c3). However, the correlation coefficients in the cross correlation are only high at a time lag of 1 hr but not at time lags of 7 and 25 hr as were observed during Section 1. The average *ef* during Section 3 was ~324 ml m^{-2} day^{-1} total gas (Figure 5c), which is much larger than the average *ef* during Sections 1 and 2. Furthermore, not only the ebullition flux but also the fraction of CH_4 in the collected gas (85%) during Section 3 was larger than during Section 1. Hence, the average flux of CH_4 due to ebullition was ~197 mg CH_4 m^{-2} day^{-1} during Section 3 and thus ~12 times larger than during Section 1.

According to the Anderson-Darling test, the ebullition fluxes within each of the three sections are not normally distributed (for each section the null hypothesis that the data originate from a population with a normal distribution was rejected: $p < 0.05$). Therefore, the nonparametric Kruskal-Wallis test was applied to assess whether the ebullition fluxes in the three sections differ. The null hypothesis that the ebullition fluxes originate from the same distribution was rejected ($p < 0.05$).

The results from the additional funnels deployed at Stations s1–s4 (see SI Figure S2) confirm the pattern between level fluctuations and ebullition fluxes observed for the different modes of operation at Station e2. Similar to the ebullition fluxes at Station e2, ebullition fluxes at Station s1 were large until 28 August and substantially lower thereafter (Figure S5s1). The ebullition fluxes at Station s3 (see SI Figure S2) show a similar pattern as the ebullition fluxes at Station e2 during modes of Operations 2 and 3, that is, ebullition fluxes were lower during September and beginning of October and large after 5 October (Figure S5s3). At Station s4 (see SI Figure S2) essentially no ebullition fluxes were observed during the entire measuring period (Figure S5s4). The water depth at Station s4 was ~31 m, and the lack of ebullition fluxes is therefore consistent with observations from July when ebullition fluxes at water column depths ≥15 m were very low (Figure 3).

4. Discussion

The main aim of this study is to investigate the effect of different reservoir operation modes on the ebullition flux of CH_4. We had the unique opportunity to assess the CH_4 ebullition flux over 4 months in a pumped-storage reservoir in which the mode of operation was changed due to maintenance work and technical modifications of the electric generation system. Initially, the reservoir was managed using a diurnal pumped-storage operation (Operation Mode 1) typical for this and many other pumped-storage systems. Later on, pumping and turbination were stopped (Operation Mode 2) and water slowly accumulated in the reservoir without substantial drawdowns. Finally, the management used the accumulated water for production of hydroelectric power by proceeding with turbination without pumping (Operation Mode 3). The ebullition flux measurements at Position e2 captured all these changes in the mode of operation at a high temporal resolution resolving subdaily time scales which allows linking diurnal and long-term changes in drawdown and water accumulation with ebullition fluxes over the 4 months of interest (Figures 4, 5, and 7). Although the additional flux measurements at other positions did not provide time series covering all modes of operation, the general findings from Station e2 are supported by these measurements (Figure S5).

Ebullition fluxes from the sediments depend on the organic material and the microbial community within the sediment, the water level affecting ambient pressure in the sediment, and on the sediment temperature effecting CH_4 production and the equilibrium gas pressure. Seasonal changes in water level and/or in water temperature may therefore cause seasonal changes in ebullition fluxes (e.g., DelSontro et al., 2010; Soja et al., 2014; Tušer et al., 2017). However, in our comparison of the ebullition fluxes during the three sections with different operation modes (Figure 4), we compare ebullition fluxes at essentially the same sediment temperature and the same daily average water level (Table 1). Ebullition fluxes between the three sections are therefore expected to be independent of seasonal effects but dominated by the consequences of the different patterns of short-term water level fluctuations associated with the different modes of operation.

The focus on a time series of ebullition flux measurements with high temporal resolution from the same station, that is, Station e2, and on time periods with the same sediment temperature and similar average water

level (selection of Sections 1–3, Figure 5) has the advantage that conclusions on the link between patterns of water level fluctuations and ebullition fluxes are neither effected by seasonal changes in abiotic conditions nor by spatial heterogeneities in microbial community or organic material within the sediment. Thus, the selected data provide an excellent basis for the investigation of the consequences of the mode of operation in pumped-storage systems for emissions by CH_4 ebullition.

The data from the different Stations s1–s4 reliably confirm our results on the link between drawdown and CH_4 ebullition fluxes during the different modes of operation. However, because the spatial distribution of ebullition fluxes of CH_4 can be very heterogeneous (Hilgert et al., 2019; Liu et al., 2020; Tušer et al., 2017), the limited spatial resolution of our ebullition flux measurements only allows for a crude estimate of the basin-wide CH_4 emissions due to ebullition. Basin-wide CH_4 emissions due to ebullition during the different modes of operation were estimated combining the information on the spatial differences in the ebullition flux from the first measurement campaign in July with the time series measured at Station e2.

In the following, we first discuss the spatial variability of ebullition fluxes and then estimate basin-wide CH_4 emissions due to ebullition. These estimates are compared to diffusive CH_4 emissions and to CH_4 emissions due to degassing during turbination and to CH_4 emissions due to ebullition observed in other studies. Thereafter, we discuss the temporal variability of the ebullition fluxes and the impact of different modes of operations on the CH_4 ebullition fluxes.

4.1. Spatial Variability of Ebullition

Ebullition fluxes decreased with increasing water column depth (Figure 3), which is consistent with previous studies (Bastviken et al., 2004; Harrison et al., 2017). At water column depths of ≥15 m, no ebullition was observed. The generation of a gas phase in the sediment requires that the equilibrium pressure of the dissolved gases in the pore water is larger than the total ambient pressure. Because hydrostatic pressure increases with water depth the generation of gas bubbles requires more net production of gas at larger than at shallower depth. Further, water and thus sediment temperature is typically higher at shallow than at large depths (Figure S6). At higher temperatures equilibrium concentrations are shifted toward the gas phase and CH_4 production is typically enhanced, both effects resulting in an increase in ebullition fluxes with increasing temperature (DelSontro et al., 2016). Hence, the likelihood to generate ebullition from sediments is smaller at large than at shallow depth. Consistently, the ebullition flux of CH_4 in Schwarzenbach reservoir is larger from sediments at shallow than at large depths (Figure 3).

4.2. Basin-Wide CH_4 Emissions Are Dominated by Ebullition Fluxes of CH_4

Basin-wide emissions of CH_4 due to ebullition were estimated by assuming that the average ebullition flux of CH_4 measured at Station e2 can be taken as estimate of the average CH_4 emission due ebullition from areas in which the water depth is shallower than 15 m (~0.21×10^6 m^2) and that no CH_4 emissions due to ebullition fluxes occur in areas with water depths larger 15 m. These assumptions are motivated by the results from the experiment in July (see section 4.1 and Figure 3) and additionally assume that the ebullition flux of CH_4 at depths less than 15 m is essentially the same as at the lake surface, which is supported by numerical analysis of CH_4-bubble fluxes (McGinnis et al., 2006). Because ebullition fluxes of CH_4 from areas with water depth <5 m are more than 2 times larger than those at e2 (see section 3.1), our estimate of the basin-wide emission of CH_4 due to ebullition must be considered as lower bound of the true basin-wide ebullition flux of CH_4. During continuous diurnal pumped-storage operation, the reservoir emitted ~3.4×10^6 mg CH_4 day^{-1} via ebullition, whereas it emitted ~4.1×10^7 mg CH_4 day^{-1} via ebullition during diurnal turbination. These ebullition fluxes are substantially larger than the diffusive emissions of CH_4 from the reservoir, that is, 4.3×10^5, 5.3×10^5, 4.8×10^5, and 1.4×10^6 mg day^{-1} determined for 14 April, 12 May, 23 June, and 18 August, respectively (Peeters et al., 2019). The diffusive CH_4 surface emissions were determined from spatial distributions of CH_4 concentrations measured at 1-m depth. Each of the four distributions was based on ~45 samples measured at different locations.

In systems, in which large amounts of CH_4 are stored in anoxic deep water, redistribution of the stored CH_4 during overturn can lead to substantial diffusive emissions of CH_4 at the water surface ("storage emission") that may contribute a major fraction of the annual diffusive emissions (Encinas Fernandez et al., 2014). However, in Schwarzenbach reservoir the deep water remained oxic throughout the year (Figure 2b) and

surface concentrations and surface fluxes of CH_4 did not increase substantially during overturn (Figure S4). At Station p1 the largest diffusive flux of CH_4 during the season was observed on 13 September when the reservoir was still stratified. The diffusive CH_4 flux decreased from 1.8 mg CH_4 m^{-2} day^{-1} on 13 September to 1.6 mg CH_4 m^{-2} day^{-1} on 29 of September to 0.7 mg CH_4 m^{-2} day^{-1} on 11 October when the water column was mixed (Figure S4). The maximum diffusive CH_4 flux was about 1 order of magnitude smaller than the ebullition flux during period 1 (16 mg CH_4 m^{-2} day^{-1}) and 2 orders of magnitude smaller than the ebullition flux during Period 3 (197 mg CH_4 m^{-2} day^{-1}), indicating that in Schwarzenbach reservoir emissions due to ebullition are substantially larger than storage emissions. Several studies have proposed that degassing of CH_4 rich water during turbination is the most important source of CH_4 emissions from reservoirs (Abril et al., 2005; Bambace et al., 2007; Kemenes et al., 2007). We estimated the CH_4 potentially released by degassing during turbination in Schwarzenbach reservoir from the volume of turbinated water, which was determined from the level decline during drawdown obtained from the pressure data and the average dissolved CH_4 concentration in the last 5 m of the water column (Figure 2) minus the CH_4 equilibrium concentration. The average CH_4 emissions due to degassing during turbination were estimated to be ~2.3×10^5 mg CH_4 day^{-1} for Section 1 and ~1.5×10^5 mg CH_4 day^{-1} for Section 3. These emissions are substantially lower than the emissions of CH_4 due to ebullition.

The analysis of the CH_4 emissions due to different processes indicates that ebullition is the dominant CH_4 emission pathway in the Schwarzenbach reservoir. In tropical reservoirs, where degassing of CH_4 during turbination was the main source of CH_4 emissions to the atmosphere (Abril et al., 2005; Bambace et al., 2007; Kemenes et al., 2007), the turbinated water was in two cases anoxic (Abril et al., 2005; Kemenes et al., 2007) and the CH_4 concentration in the turbinated water was in all cases much higher than in Schwarzenbach reservoir. The dominance of CH_4 emissions by ebullition observed in Schwarzenbach reservoirs agrees well with observations from other temperate reservoirs where ebullition is also the main pathway of CH_4 emissions to the atmosphere (DelSontro et al., 2010).

4.3. Comparisons of the CH_4 Emission by Ebullition With Observations in Other Systems

According to a recent synthesis of GHG emissions from reservoirs (Deemer et al., 2020), the average emission via ebullition of reservoirs with hydropower capacity is ~98 mg CH_4 m^{-2} day^{-1} (~0.43 to ~591.62 mg CH_4 m^{-2} day^{-1}). The estimates of the basin-wide emissions from Schwarzenbach reservoir were ~3.4×10^6 mg CH_4 day^{-1} during continuous diurnal pumped-storage operations (Section 1) and ~4.1×10^7 mg CH_4 day^{-1} during diurnal turbination (Section 3). The corresponding basin-wide emissions per unit surface area are ~5.6 and 62 mg CH_4 m^{-2} day^{-1}, respectively, for these two modes of operation. Hence, the emissions due to ebullition from Schwarzenbach reservoir are at the lower end of those for the hydropower reservoirs compiled by Deemer et al. (2020). The comparatively low ebullition fluxes may be related to the rather shallow sediments in the reservoir, the recent complete drainage of the reservoir in 1997, or the low alkalinity of the water (0.2 mmol L^{-1}).

Our observation that ebullition fluxes increase substantially when drawdown occurs after a time period without drawdowns (Operation Modes 2 and 3 in Figure 4) is consistent with observations in several reservoirs which were operated with a single major annual drawdown in fall (Harrison et al. (2017). Also in natural systems, for example, the Amazon floodplains, CH_4 ebullition fluxes become large when the water level drops after an extended time period of water level rise (Engle & Melack, 2000). The average ebullition flux of CH_4 for all reservoirs studied by Harrison et al. (2017) was 42 mg CH_4 m^{-2} day^{-1} (range 0.0–192.6 mg CH_4 $m^{-2}day^{-1}$) during predrawdown time periods and increased by a factor of 5 to 223 mg CH_4 m^{-2} day^{-1} (range 0.09–719 mg CH_4 m^{-2} day^{-1}) during drawdown periods and thus to values larger than the average CH_4 ebullition flux for hydropower reservoirs reported by Deemer et al. (2020).

The study by Harrison et al., 2017 includes 5 days of observations from J.C. Boyle reservoir during which daily drawdowns occurred. As in Schwarzenbach reservoir daily drawdowns were associated with pulsed release of CH_4-rich bubbles from the sediment (Harrison et al., 2017). During the ~5 days evaluated, the reservoir emitted ~720 (±398) mg CH_4 m^{-2} day^{-1}, more than an order of magnitude more CH_4 than Schwarzenbach reservoir. The very high ebullition fluxes of CH_4 from J.C. Boyle reservoir are probably related to high CH_4 production in the sediments, as the temperature of the bottom water is ~19.71°C and the ebullition flux of CH_4 during no-drawdown periods is ~193 ± 107 mg CH_4 m^{-2} day^{-1} and thus larger

than in the other six reservoirs investigated by Harrison et al. (2017) and also 2 times larger than the average CH_4 ebullition flux from the hydropower reservoirs considered by Deemer et al. (2020). The duration of daily drawdown in the J.C. Boyle reservoir was ~10 hr and thus much longer than in the Schwarzenbach reservoir which has contributed to the very high CH_4 ebullition fluxes during drawdown periods.

4.4. Effect of Different Modes of Operation on CH_4 Ebullition

Despite several investigations providing information of CH_4 ebullition fluxes from reservoirs, the consequences of different modes of operation in a pumped-storage hydropower reservoir on CH_4 ebullition fluxes have, to our knowledge, not yet been studied in detail. Our investigation in Schwarzenbach reservoir includes three time periods that resemble conditions during three different types of reservoir operation (Figures 5a1–5a3). During Section 1, the reservoir is operated in a diurnal pump-turbination mode which is typical for pumped-storage hydropower generation. This mode of operation causes diurnal increases and decreases in water level (Figure 5a1). A similar pumped-storage operation was performed every day, as is indicated by the positive *wlc* autocorrelation at a time lag of 24 hr (Figure 7a1). The negative *wlc* autocorrelation at a time lag of 6 hr (Figure 7a1) suggests that pumping starts 6 hr after turbination, that is. the water is discharged via the turbines and pumped back from Kirschbaumwasen after 6 hr. The ebullition fluxes from the sediment during Section 1 predominantly occurred during periods of water level drawdown (Figure 6b1). The time lag of the negative cross correlation between the *ef* and the *wlc* of about −1 hr (Figure 7b1) suggests that the ebullition flux is maximal shortly after the maximum rate of water level decrease. The data show also a diurnal cycle in ebullition fluxes from the sediment (Figure 7b1) that agrees with the diurnal change in water level (Figure 7c1). The ~7-hr lag in the positive cross correlation between *ef* and *wlc* (Figure 7c1) results from the 6-hr difference between maximum rate of water level decrease due to turbination and the maximum water level increase due to pumping. Because *ef* occurs mainly during the decrease in water level, the 6-hr lag leads to negative autocorrelations in *wlc* (negative *wlc* versus positive *wlc*) but positive cross correlation (positive *wlc* versus positive *ef*) at ~7-hr lag.

Section 2 is characterized by a constant increase in the water level (Figure 5a2) caused by the mode of operation during this period which did not include turbination and therefore no water level drawdowns. Thus, during Section 2 the ebullition flux was negligible (Figure 5c), that is, ~200 times smaller than during Section 1 (diurnal pumping and turbination operation).

During Section 3, reservoir management aimed at production of hydropower from the water stored during the previous section and therefore performed intensive turbination. Thus, drawdowns dominated the changes in water level (Figure 5a3). Unlike during Section 1 (Figure 7a1), the *wlc* during Section 3 did not show a significant positive autocorrelation at any time lag (apart of the 0-hr lag; Figure 7c1), which indicates that turbination was not conducted periodically. As in Section 1, the ebullition fluxes from sediments showed a significant negative cross correlation with the rate of change in water level (Figure 7c3), which is consistent with the conclusion that the water drawdown caused by the turbination triggers ebullition fluxes. During Section 3, ebullition fluxes from sediments did not occur periodically (Figures 7c2 and 7c3) which is consistent with nonperiodic changes in water level and thus the reservoir management.

Turbination causes a drawdown in water level, and the associated decrease in hydrostatic pressure at the sediment is the main mechanism that triggers ebullition. This is supported by the correlation analysis (Figure 7) and by the observation that ebullition fluxes were substantially larger (Figure 5c) during modes of operation with turbination (Sections 1 and 3) than without turbination (Section 2; significant differences between the three sections based on the Kruskal-Wallis test, p value <0.05). However, CH_4 ebullition fluxes varied substantially between the different modes of operation that included turbination. During continuous diurnal pumped-storage operation (Section 1) CH_4 ebullition fluxes were ~12 times smaller than during diurnal turbination (Section 3) that followed a time period of no pumping and no turbination (Section 2). The amount of gas emitted as bubbles and also the CH_4 concentration within this gas are larger during Section 3 than during the other two sections (1 and 2) indicating that the management of the reservoir has an effect on the ebullition flux and the associated CH_4 emissions. Between 28 August and 5 October, ebullition was minimal because turbination was stopped and water level did not show diurnal fluctuations but increased over time (Figure 4; see also Section 2 in Figure 5). During this time period, CH_4 was not regularly removed from the sediment by ebullition as it was the case for example, during Section 1. Hence, from

28 August onward until 5 October CH_4 production probably resulted in the accumulation of CH_4 and thus in an increase in the partial pressure of CH_4 within the sediments. When turbination was resumed on 5 October, CH_4 concentrations in the sediment most likely were substantially oversaturated supporting bubble formation and large ebullition fluxes at decreasing hydrostatic pressure associated with the mode of operation consisting of regular turbination without pumping for water storage.

The accumulation of CH_4 in the sediment during the time period of no turbination may explain why ebullition fluxes and CH_4 concentrations in the emitted gas were substantially larger during Section 3 than during Section 1. The continuous diurnal pump-turbination mode of operation during Section 1 caused diurnally short ebullition events regularly removing CH_4 from the sediments thus preventing a substantial accumulation of CH_4 in the pore water. Hence, the partial pressure of CH_4 in the pore water most likely was substantially larger during Section 2 than during Section 1. Increased partial pressure of CH_4 in the pore water prior to bubble release not only explains that a decline in hydrostatic pressure due to turbination triggered larger ebullition fluxes during Section 3 but also that the fraction of CH_4 in the gas bubbles was larger during Section 3 than during Section 1. Increased CH_4 concentration in the gas at larger ebullition fluxes was also observed in Lacamas Lake (Harrison et al., 2017). Harrison et al. (2017) reported a fraction of ~61% CH_4 in the gas of bubbles released from the sediments during drawdowns but only ~30% CH_4 during no-drawdown periods. Moreover, a positive log linear relationship was found between ebullition flux and bubble CH_4 concentrations (Harrison et al., 2017), suggesting an increased sediment-to-atmosphere transfer efficiency for CH_4 in bubbles emitted during drawdown due to larger bubble sizes and/or higher sediment or water column CH_4 concentrations.

The ebullition fluxes quantified for the three sections with the three different modes of operation suggest that a reservoir management using continuous diurnal pumped-storage operation over 100 days causes essentially the same CH_4 emissions due to ebullition (~1,600 mg m^{-2} CH_4) as a management that uses ~92 days of no turbination followed by ~8 days of diurnal turbination. The latter type of reservoir management, that is, no turbination over an extended time period followed by drawdowns over several days is typical for many reservoirs used for purposes such as flood prevention, recreational uses, water supply, or even hydroelectric power generation (Harrison et al., 2017).

The conclusion that a reservoir operation using no turbination over an extended time period followed by water drawdown over several days leads to a larger average CH_4 ebullition flux than continuous diurnal pumped-storage operation is based on the data from the three, 5-day long, selected sections (Figure 5). However, a very similar conclusion is obtained if the analysis is based on the CH_4 ebullition fluxes measured during the 51-day long time period from 28 August until 18 October. During this time period, which combines the time period of CH_4 accumulation in the sediment between 28 August and 5 October with the drawdown period thereafter until 18 October, the average CH_4 emission from the sediment by ebullition was ~36 mg CH_4 m^{-2} day^{-1}. This average CH_4 ebullition flux assumes that the molar fraction of CH_4 in the gas bubbles was 42% (as in Section 1) until 5 October and was 85% (as in Section 3) after 5 October. Note that the average CH_4 ebullition flux of ~36 mg CH_4 m^{-2} day^{-1} is an underestimation because it does not include the time periods with missing data (Figure 4b). Assuming that during the data gaps from 18 to 24 September and from 14 to 17 October CH_4 fluxes correspond to the average CH_4 fluxes measured during Sections 2 and 3, respectively, the average CH_4 ebullition flux for the continuous time period from 28 August to 18 October increases to ~46 mg CH_4 m^{-2} day^{-1}. This value is ~2.8 times larger than the average CH_4 ebullition flux during Section 1 (~16 mg CH_4 m^{-2} day^{-1}) that is characteristic for CH_4 ebullition fluxes during diurnal pumped-storage operation (Operation Mode 1).

The results from the analysis imply that during 51 days of continuous diurnal pumped-storage operation, the CH_4 flux due to ebullition is ~831 mg CH_4 m^{-2}, which is only ~35.7% of the CH_4 ebullition flux released by a 51-day reservoir operation that uses 38 days of no turbination followed by 13 days of diurnal turbination (~2,325 mg CH_4 m^{-2}).

Hence, reservoir management aiming at a continuous diurnal pumped-storage operation supports a reduction of CH_4 ebullition fluxes compared to management strategies that use longer-term time periods of no turbination followed by intensive turbination over several days.

Our study shows that pumped-storage systems cause emissions of the potent GHG CH_4 by ebullition. The typical mode of operation in pumped-storage hydropower reservoirs, that is, turbination and pumping at subdiel time scales, is however a good means to keep CH_4 emissions due to ebullition at a comparatively low level. In reservoirs used for other purposes than hydropower generation that typically do not use a subdiel pumped-storage operation, regular smaller drawdowns instead of single massive draw down at the end of the season may be advantageous to reduce methane emissions.

5. Conclusions

Our results show that water level drawdown associated with turbination triggers CH_4 ebullition from the sediment and that the mode of operation of the reservoir has a substantial influence on the ebullition fluxes of CH_4 from the reservoir. The data suggest that continuous diurnal pumped-storage operation causing short drawdowns and water level restoration at a diel or subdiel cycle results in smaller CH_4 emissions by ebullition from the sediments than management strategies aiming at the accumulation of water over an extended time period followed by intensive turbination over several days. Because ebullition is in many cases the dominant pathways of overall CH_4 emissions from reservoirs to the atmosphere (DelSontro et al., 2010; Sobek et al., 2012) and CH_4 is a very potent GHG, adopting a management strategy of continuous diurnal pumped-storage operation will contribute to a reduction of GHG emissions from reservoirs.

Data Availability Statement

All data and information relevant to this article will be made available before publication.

Acknowledgments

We thank Joseph Halder, Beatrix Rosenberg, Christopher Igel, and many student assistants for their help and support in the field and in the lab. We thank Dr. Franke and the EnBW team working at the Schwarzenbach reservoir for their support and H. Wunsch for the wind data from the reservoirs. The work was financially supported by the Ministry of Science, Research and the Arts of the Federal State Baden-Württemberg, Germany (Grant: Water Research Network project: Challenges of Reservoir Management-Meeting Environmental and Social Requirements).

References

Abril, G., Guérin, F., Richard, S., Delmas, R., Galy-Lacaux, C., Gosse, P., et al. (2005). Carbon dioxide and methane emissions and the carbon budget of a 10-year old tropical reservoir (Petit Saut, French Guiana). *Global Biogeochemical Cycles*, *19*, GB4007. https://doi.org/10.1029/2005GB002457

Bambace, L. A. W., Ramos, F. M., Lima, I. B. T., & Rosa, R. R. (2007). Mitigation and recovery of methane emissions from tropical hydroelectric dams. *Energy*, *32*(6), 1038–1046. https://doi.org/10.1016/j.energy.2006.09.008

Barbour, E., Wilson, I. A. G., Radcliffe, J., Ding, Y., & Li, Y. (2016). A review of pumped hydro energy storage development in significant international electricity markets. *Renewable and Sustainable Energy Reviews*, *61*, 421–432. https://doi.org/10.1016/j.rser.2016.04.0

Barros, N., Cole, J. J., Tranvik, L. J., Prairie, Y. T., Bastviken, D., Huszar, V. L. M., et al. (2011). Carbon emission from hydroelectric reservoirs linked to reservoir age and latitude. *Nature Geoscience*, *4*(9), 593–596. https://doi.org/10.1038/ngeo1211

Bastviken, D., Cole, J., Pace, M., & Tranvik, L. (2004). Methane emissions from lakes: Dependence of lake characteristics, two regional assessments, and a global estimate. *Global Biogeochemical Cycles*, *18*, GB4009. https://doi.org/10.1029/2004GB002238

Bastviken, D., Cole, J. J., Pace, M. L., & Van de Bogert, M. C. (2008). Fates of methane from different lake habitats: Connecting whole-lake budgets and CH4 emissions. *Journal of Geophysical Research*, *113*, G02024. https://doi.org/10.1029/2007JG000608

Bastviken, D., Ejlertsson, J., & Tranvik, L. (2002). Measurement of methane oxidation in lakes: A comparison of methods. *Environmental Science & Technology*, *36*(15), 3354–3361. https://doi.org/10.1021/es010311p

Bastviken, D., Tranvik, L., Downing, J., Crill, P., & Enrich-Prast, A. (2011). Freshwater methane emissions offset the continental carbon sink. *Science*, *331*(6013), 50. https://doi.org/10.1126/science.1196808

Battin, T., Luyssaert, S., Kaplan, L., Audfenkampe, A., Richter, A., & Tranvik, L. (2009). The boundless carbon cycle. *Nature Geoscience*, *2*(9), 598–600. https://doi.org/10.1038/ngeo618

Beaulieu, J. J., Smolenski, R. L., Nietch, C. T., Townsend-Small, A., & Elovitz, M. S. (2014). High methane emissions from a midlatitude reservoir draining an agricultural watershed. *Environmental Science & Technology*, *48*(19), 11,100–11,108. https://doi.org/10.1021/es501871g

Clow, D. W., Stackpoole, S. M., Verdin, K. L., Butman, D. E., Zhu, Z., Krabbenhoft, D. P., & Striegl, R. G. (2015). Organic carbon burial in lakes and reservoirs of the conterminous United States. *Environmental Science & Technology*, *49*(13), 7614–7622. https://doi.org/10.1021/acs.est.5b00373

Cole, J. J., & Caraco, N. F. (1998). Atmospheric exchange of carbon dioxide in a low-wind oligotrophic lake measured by the addition of SF6. *Limnology and Oceanography*, *43*(4), 647–656. https://doi.org/10.4319/lo.1998.43.4.0647

Commission (2011). *Energy roadmap 2050. Com, 885*. Brussels, Belgium: EU Commision.

Deane, J. P., Ó Gallachóir, B. P., & McKeogh, E. J. (2010). Techno-economic review of existing and new pumped hydro energy storage plant. *Renewable and Sustainable Energy Reviews, Elsevier*, *14*(4), 1293–1302. https://doi.org/10.1016/j.rser.2009.11.015

Deborde, J., Anschutz, P., Guérin, F., Poirier, D., Marty, D., Boucher, G., et al. (2010). Methane sources, sinks and fluxes in a temperate tidal Lagoon: The Arcachon lagoon (SW France). *Estuarine, Coastal and Shelf Science, Elsevier*, *89*, 256–266. https://doi.org/10.1016/j.ecss.2010.07.013

Deemer, B. R., Harrison, J. A., Li, S., Beaulieu, J. J., DelSontro, T., Barros, N., et al. (2016). Greenhouse gas emissions from reservoir water surfaces: A new global synthesis. *BioScience*, *66*(11), 949–964. https://doi.org/10.1093/biosci/biw117

Deemer, B. R., Harrison, J. A., Li, S., Beaulieu, J. J., DelSontro, T., Barros, N., et al. (2020). Data from: Greenhouse gas emissions from reservoir water surfaces: A new global synthesis, v2. In *Dryad*. Dataset. https://doi.org/10.5061/dryad.d2kv0

DelSontro, T., Boutet, L., St-Pierre, A., del Giorgio, P. A., & Praire, Y. T. (2016). Methane ebullition and diffusion from northern ponds and lakes regulated by the interaction between temperature and system productivity. *Limnology and Oceanography*, *61*(S1), S62–S77. https://doi.org/10.1002/lno.10335

DelSontro, T., McGinnis, D. F., Sobek, S., Ostrovsky, I., & Wehrli, B. (2010). Extreme methane emissions from a Swiss hydropower reservoir: Contribution from bubbling sediments. *Environmental Science & Technology*, *44*(7), 2419–2425. https://doi.org/10.1021/es9031369

Encinas Fernandez, J., Peeters, F., & Hofmann, H. (2014). Importance of the autumn overturn and anoxic conditions in the hypolimnion for the annual methane emissions from a temperate lake. *Environmental Science & Technology*, *48*(13), 7297–7304. https://doi.org/10.1021/es4056164

Engle, D., & Melack, J. M. (2000). Methane emissions from an Amazon floodplain lake: Enhanced release during episodic mixing and during falling water. *Biogeochemistry*, *51*(1), 71–90. https://doi.org/10.1023/A:1006389124823

Harrison, J. A., Deemer, B. R., Birchfield, M. K., & O'Malley, M. T. (2017). Reservoir water-level drawdowns accelerate and amplify methane emission. *Environmental Science & Technology*, *51*(3), 1267–1277. https://doi.org/10.1021/acs.est.6b03185

Hayes, N. M., Deemer, B. R., Corman, J. R., Razavi, N. R., & Strock, K. E. (2017). Key differences between lakes and reservoirs modify climate signals: A case for a new conceptual model. *Limnology and Oceanography Letters*, *2*(2), 47–62. https://doi.org/10.1002/lol2.10036

Hertwich, E. G. (2013). Addressing biogenic greenhouse gas emissions from hydropower in LCA. *Environmental Science & Technology*, *47*(17), 9604–9611. https://doi.org/10.1021/es401820p

Hilgert, S., Sotiri, K., Marcon, L., Liu, L., Bleninger, T., Mannich, M., & Fuchs, S. (2019). Resolving spatial heterogeneities of methane ebullition flux from a Brazilian reservoir by combining hydro-acoustic measurements with methane production potential. In *38th international association of hydro resources world congress, Panama City, Panama* (pp. 3576–3585). International organization: IAHR World Congress. https://doi.org/10.3850/38WC092019-0866

Hoffert, M. I., Caldeira, K., Jain, A. K., Haites, E. F., Harvey, L. D., Potter, S. D., et al. (1998). Energy implications of future stabilization of atmospheric CO_2 content. *Nature*, *395*(6705), 881–884. https://doi.org/10.1038/27638

Hofmann, H., Federwisch, L., & Peeters, F. (2010). Wave-induced release of methane: Littoral zones as a source of methane in lakes. *Limnology and Oceanography*, *55*(5), 1990–2000. https://doi.org/10.4319/lo.2010.55.5.1990

Ibrahim, H., Ilinca, A., & Perron, J. (2008). Energy storage systems—Characteristics and comparisons. *Renewable and Sustainable Energy Reviews*, *12*(5), 1221–1250. https://doi.org/10.1016/j.rser.2007.01.023

Joyce, J., & Jewell, P. W. (2003). Physical controls on methane ebullition from reservoirs and lakes. *Environmental and Engineering Geoscience*, *9*(2), 167–178. https://doi.org/10.2113/9.2.167

Kemenes, A., Forsberg, B. R., & Melack, J. M. (2007). Methane release below a tropical hydroelectric dam. *Geophysical Research Letters*, *34*, L12809. https://doi.org/10.1029/2007GL029479

Kobler, U. G., Wüest, A., & Schmid, M. (2019). Combined effects of pumped-storage operation and climate change on thermal structure and water quality. *Climatic Change*, *152*(3–4), 413–429. https://doi.org/10.1007/s10584-018-2340-x

Lima, I. B. T., da Silva Ramos, F. M., Waack Bambace, L. A., & Rosa, R. R. (2007). Methane emissions from large dams as renewable energy resources: A developing nation perspective. *Mitigation and Adaptation Strategies for Global Change*, *13*(2), 193–206. https://doi.org/10.1007/s11027-007-9086-5

Liss, P. S., & Merlivat, L. (1986). Air-sea gas exchange rates: Introduction and synthesis. In *The role of air—sea exchange in geochemical cycling* (pp. 113–127). Dordrecht, The Netherlands: D. Reidel, Publishing Company. https://doi.org/10.1007/978-94-009-4738-2_5

Liu, L., Yang, Z. J., Delwiche, K., Long, L. H., Liu, J., Liu, D. F., et al. (2020). Spatial and temporal variability of methane emissions from cascading reservoirs in the Upper Mekong River. *Water Research*, *186*, 116319. https://doi.org/10.1016/j.watres.2020.116319

Luyssaert, S., Abril, G., Andres, R., Bastviken, D., Bellassen, V., Bergamaschi, P., et al. (2012). The European land and inland water CO_2, CO, CH_4 and N_2O balance between 2001 and 2005. *Biogeosciences*, *9*(8), 3357–3380. https://doi.org/10.5194/bg-9-3357-2012

Maeck, A., Hofmann, H., & Lorke, A. (2014). Pumping methane out of aquatic sediments—Ebullition forcing mechanisms in an impounded river. *Biogeosciences*, *11*(11), 2925–2938. https://doi.org/10.5194/bg-11-2925-2014

McGinnis, D. F., Greinert, J., Artemov, Y., Beaubien, S. E., & Wüest, A. (2006). Fate of rising methane bubbles in stratified waters: How much methane reaches the atmosphere? *Journal of Geophysical Research*, *111*, C09007. https://doi.org/10.1029/2005JC003183

Mendonça, R., Müller, R. A., Clow, D., Verpoorter, C., Raymond, P., Tranvik, J. L., & Sobek, S. (2017). Organic carbon burial in global lakes and reservoirs. *Nature Communications*, *8*(1), 1694. https://doi.org/10.1038/s41467-017-01789-6

Ostrovsky, I., McGinnis, D. F., Lapidus, L., & Eckert, W. (2008). Quantifying gas ebullition with echosounder: The role of methane transport by bubbles in a medium-sized lake. *Limnology and Oceanography: Methods*, *6*(2), 105–118. https://doi.org/10.4319/lom.2008.6.105

Peeters, F., Encinas Fernandez, J., & Hofmann, H. (2019). Sediment fluxes rather than oxic methanogenesis explain diffusive CH_4 emissions from lakes and reservoirs. *Scientific Reports*, *9*(1), 243. http://doi.org/10.1038/s41598-018-36530-w

Phyoe, W. W., & Wang, F. (2019). A review of carbon sink or source effect on artificial reservoirs. *International journal of Environmental Science and Technology*, *16*(4), 2161–2174. https://doi.org/10.1007/s13762-019-02237-2

Raymond, P. A., Hartmann, J., Lauerwald, R., Sobek, S., McDonald, C., Hoover, M., et al. (2013). Global carbon dioxide emissions from inland waters. *Nature*, *503*(7476), 355–359. https://doi.org/10.1038/nature12760

Rehman, S., Al-Hadhrami, L. M., & Alam, M. M. (2015). Pumped hydro energy storage system: A technological review. *Renewable and Sustainable Energy Reviews, Elsevier*, *44*(C), 586–598. https://doi.org/10.1016/j.rser.2014.12.040

REN21 (2017). *Renewables 2017 global status report*. Paris: REN21 Secretariat.

Scandella, B. P., Varadharajan, C., Hemond, H. F., Ruppel, C., & Juanes, R. (2011). A conduit dilation model of methane venting from lake sediments. *Geophysical Research Letters*, *38*, L06408. https://doi.org/10.1029/2011GL046768

Sobek, S., DelSontro, T., Wongfun, N., & Wehrli, B. (2012). Extreme organic carbon burial fuels intense methane bubbling in a temperate reservoir. *Geophysical Research Letters*, *39*, L01401. https://doi.org/10.1029/2011GL050144

Soja, G., Kitzler, B., & Soja, A.-M. (2014). Emissions of greenhouse gases from Lake Neusiedl, a shallow steppe lake in Eastern Austria. *Hydrobiologia*, *731*(1), 125–138. https://doi.org/10.1007/s10750-013-1681-8

Tranvik, L. J., Downing, J. A., Cotner, J. B., Loiselle, S. A., Striegl, R. G., Ballatore, T. J., et al. (2009). Lakes and reservoirs as regulators of carbon cycling and climate. *Limnology and Oceanography*, *54*(6part2), 2298–2314. https://doi.org/10.4319/lo.2009.54.6_part_2.2298

Tušer, M., Picek, T., Sajdlová, Z., Juza, T., Muška, M., & Frouzová, J. (2017). Seasonal and spatial dynamics of gas ebullition in a temperate water storage reservoir. *Water Resources Research*, *53*, 8266–8276. https://doi.org/10.1002/2017WR020694

Varadharajan, C., & Hemond, H. F. (2012). Time-series analysis of high-resolution ebullition fluxes from a stratified, freshwater lake. *Journal of Geophysical Research*, *117*, G02004. https://doi.org/10.1029/2011JG001866

Victor, D. G. (1998). Global warming: Strategies for cutting carbon. *Nature*, *395*(6705), 837–838. https://doi.org/10.1038/27532

Zohary, T., & Ostrovsky, I. (2011). Ecological impacts of excessive water level fluctuations in stratified freshwater lakes. *Inland Waters*, *1*(1), 47–59. https://doi.org/10.5268/IW-1.1.406